Journal of the Physical Society of Japan
Vol. 76, No. 3, March, 2007, 033704

Magnetic Study of Pressure-Induced Superconductivity in the [Pd(dmit)$_2$] Salt with Spin-Gapped Ground State

Yasuyuki ISHII, Masafumi TAMURA, and Reizo KATO

Condensed Molecular Materials Laboratory, RIKEN, 2-1 Hirosawa, Wako, Saitama 351-1098

(Received October 13, 2006; accepted January 10, 2007; published February 26, 2007)

Static magnetic measurements have been applied for the pressure-induced superconducting state in the $P2_1/m$ phase of $EtMe_3P[Pd(dmit)_2]_2$ (Et = C_2H_5, Me = CH_3 and $dmit^{2-}$ = 1,3-dithiol-2-thione-4,5-dithiolate, $C_3S_5^{2-}$), which exhibits valence bond (VB) ordering with a spin gap at ambient pressure. Evidence for bulk superconductivity is given. The pressure dependence of the transition temperature (T_c) is obtained in the pressure range 0.2–0.5 GPa. A possible relation between the VB order and the superconductivity is suggested on the basis of the phase diagram. The nonlinear magnetization process is analyzed to determine the behavior of the lower critical field (H_{c1}).

KEYWORDS: Pd(dmit)$_2$, superconductivity, pressure, triangular antiferromagnet, valence bond order, magnetic susceptibility
DOI: 10.1143/JPSJ.76.033704

A series of radical anion salts of the metal complex molecule [Pd(dmit)$_2$] manifests unconventional physical behavior related to frustrated quantum spins.[1–4] The frustration arises from the two-dimensional (2D) triangular network of the dimeric units [Pd(dmit)$_2$]$_2$ within the crystallographic *ac* plane. At ambient pressure, they are Mott insulators, in which each $S = 1/2$ spin is localized on each dimer.[1–5] The strength of the frustration in the [Pd(dmit)$_2$] salts, as regulated by the spatial anisotropy of the triangular exchange network, can be experimentally controlled by the choice of counter cation.[1–4] Furthermore, using the pressure or strain effect on the [Pd(dmit)$_2$] salts, we can explore the effects of the frustration and the electron correlation systematically.[4,6,7]

We have recently found a VB-ordered state in the $P2_1/m$ phase of $EtMe_3P[Pd(dmit)_2]$ (the $P2_1/m$ $EtMe_3P$ salt) below 25 K.[6,8] Similarly to the spin-Peierls transition, this VB ordering is accompanied by the spin gap and lattice translational symmetry breaking.[6,8] The frustration, diminishing the antiferromagnetic long-range order, leads the quantum spins to the VB formation in spite of the 2D character.[6] The VB ordering can be suppressed by pressure, because it is accompanied by volume expansion. Interestingly, superconductivity appears in the proximity of the VB-ordered phase, as mentioned in refs. 8 and 9. This finding has prompted us to study the possible role of the VB formation (real-space pairing of electrons) underlying the superconductivity. The spin correlation leading to the VB formation has been a clue to understand the physics behind the strongly correlating electron systems such as high-T_c superconductors, as first proposed by Anderson.[10]

In this paper, we report the macroscopic magnetic characterization of the pressure-induced superconductivity in the $P2_1/m$ $EtMe_3P$ salt. The [Pd(dmit)$_2$] family have provided several superconductors under pressure (in 0.5–1 GPa range) so far.[4] However, the volume fraction is generally too small; no bulk diamagnetic signal has been detected,[11] in spite of the transport properties showing an anisotropic field effect related to the crystal axes.[4,12,13] Therefore, macroscopic characterization of the superconductivity is immensely desired for these materials, prior to examining its origin. For the $P2_1/m$ $EtMe_3P$ salt, contrastingly, we have succeeded in showing bulk superconductivity in the $P2_1/m$ $EtMe_3P$ salt by static magnetic measurements for the sample under pressure. The pressure dependence of T_c has been obtained. From the analysis of the magnetization (M) curve, we have estimated the lower critical field H_{c1} values for the field applied perpendicular to the 2D plane.

Black plate-like crystals of the $P2_1/m$ $EtMe_3P$ salt were prepared as described elsewhere.[9] The most developed crystal face is the *ac*-plane, in which the [Pd(dmit)$_2$] dimers have a 2D arrangement. In this paper, we use the crystal axis notation for the room temperature structure.[5,9] Hydrostatic pressure was applied using a clamp-type piston cylinder cell designed for magnetic measurements. Daphne 7373 oil (Idemitsu Oil & Gas) was used as a pressure-transmitting medium. A polycrystalline (randomly oriented small crystals) or a single-crystal sample was placed in a cylindrical capsule installed between two spacer rods in the pressure cell. The sample capsule and the spacer rods were made of a fluorocarbon plastic. The dc-magnetization characteristics were measured using a SQUID magnetometer (Quantum Design MPMS XL7). The pressure at low temperatures was monitored at each run by the shift of T_c for a small Pb piece set in the cell. This simple method gives a satisfactorily reliable estimation of pressure at low temperatures.

Figure 1(a) shows the temperature dependence of susceptibility $\chi(T)$ at selected pressures. The VB ordering is suppressed by pressure, as mentioned previously.[6,8] Whereas it is observed at 25 K under ambient pressure, it appears at 16 K under 0.21 GPa.[6] Superconductivity appears slightly below this pressure. The superconducting transition temperature T_c, as determined by the onset of the diamagnetic signal, is 4.8 K at 0.18 GPa [Fig. 1(b)]. The pressure dependence of T_c is shown in Fig. 1(c), together with that of the VB ordering temperature. Near the critical pressure, *ca.* 0.15 GPa, we could observe a weak diamagnetic signal suggesting the coexistence of SC and insulating phases. On the low-pressure side of the superconducting phase, the phase boundary seems to be vertical. We surmise that the insulator-to-superconductor transition is a first-order one, taking account of the third law of thermodynamics. In the narrow pressure range near 0.2 GPa, resistivity measurements upon lowering the temperature have revealed insu-

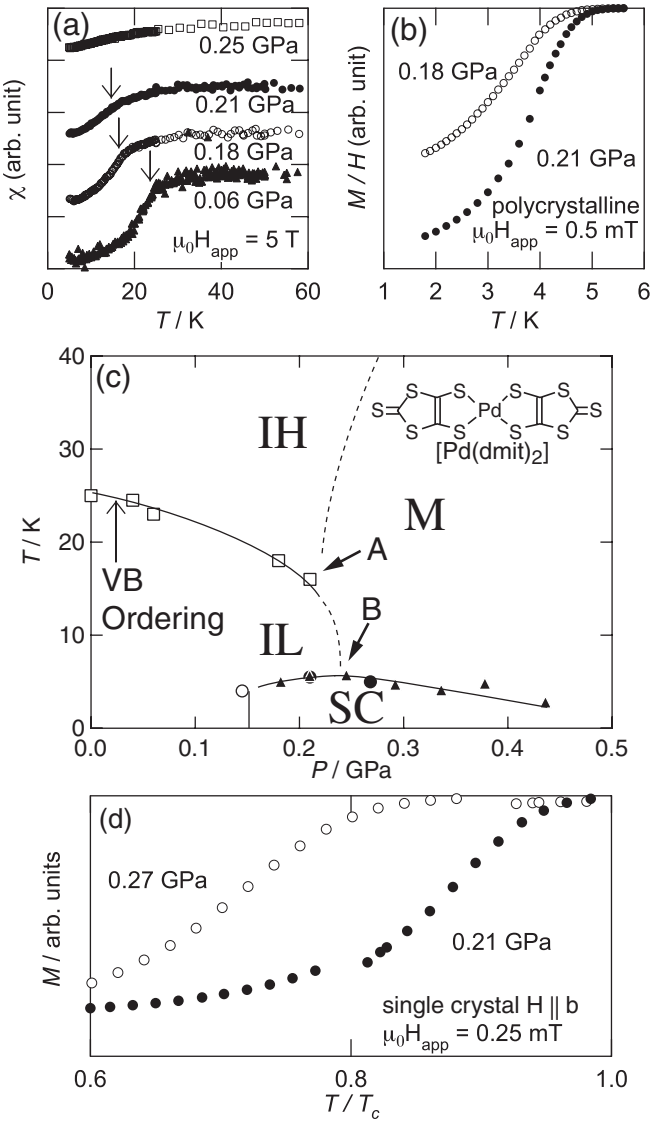

Fig. 1. (a) Low-temperature part of the χ vs T curves for polycrystalline sample of the $P2_1/m$ $EtMe_3P$ salt for selected pressures.[6] (b) Diamagnetic signal for the polycrystalline sample at low temperatures. (c) Temperature–pressure phase diagram for the $P2_1/m$ $EtMe_3P$ salt. The curve for the VB ordering is based on the susceptibility measurements for the polycrystalline samples (□).[6] The diamagnetic onset T_c is determined for the polycrystalline (▲) and single-crystal data (●). The open circle indicates T_c for the inhomogeneous case near the boundary. The IH–M boundary (dashed curve) is drawn according to the resistivity measurements.[9,14] (d) Magnetization of the single crystal vs normalized temperature at 0.21 and 0.27 GPa, with a field of 0.25 mT applied along the b direction.

lator–metal–insulator–superconductor (IH–M–IL–SC) successive phase transitions.[9,14] The low-temperature insulating phase IL corresponds to the ordered phase, whereas the IH phase is paramagnetic. Unlike the conventional [Pd(dmit)$_2$] salts, the M phase penetrates to the low-temperature side of the IH phase, suggesting that the IH phase has a large entropy due to the frustration. The penetration is limited by the ordered phase IL, whose entropy should be small. Near the boundary between the IL and M phases, T_c, as determined by the diamagnetic onset, seems to take a maximum, $T_c = 5.5$ K at 0.2 GPa. It gradually decreases to *ca.* 3 K as pressure is increased to 0.44 GPa, and the resistivity measurements show IH–M–SC transitions in this region.[4] The pressure dependence of T_c appears weak. However, the effect of pressure is more evident in the temperature dependence of the diamagnetic signal [Fig. 1(d)]. The growth of the diamagnetic signal below T_c becomes slow by pressurization. This can be related to the anomalous behavior of H_{c1} near T_c, which will be mentioned below. The superconductivity rapidly disappears above 2 K as 0.5 GPa is approached.

The bulk diamagnetic signal is observed at pressures below and above the IL–M boundary near 0.24 GPa [Fig. 1(d)]. The present results indicate that the SC phase distinctly penetrates the low-temperature side of the spin-gapped IL phase. The almost pressure-independent T_c at around B implies the first-order nature of the SC transition, which can be justified from a macroscopic viewpoint. The first-order IL–M transition can be observed only within a considerably narrow pressure range (A–B) by resistivity measurements.[9,14] This means that the IL–M transition involves little entropy change. On the IL–M boundary, we write the changes in the volume and entropy as $V_{IL} = V_M + (\Delta V)_{IL-M}$ and $S_{IL} = S_M + (\Delta S)_{IL-M}$, respectively, where V_{IL} is the molar volume of the IL phase and so on. The Clausius–Clapeyron relation gives the reciprocal slope of the boundary as $(dP/dT)_{IL-M} = (\Delta S)_{IL-M}/(\Delta V)_{IL-M} \lesssim 0$. It follows that $(\Delta S)_{IL-M} \lesssim 0$ (a small negative value) and $(\Delta V)_{IL-M} > 0$. Assuming the first-order IL–SC boundary, we obtain $(dP/dT)_{IL-SC} = (S_{IL} - S_{SC})/(V_{IL} - V_{SC}) \simeq (\Delta S)_{M-SC}/(\Delta V)_{IL-M} + (dP/dT)_{IL-M}$, where $(\Delta S)_{M-SC} = S_M - S_{SC} = S_{IL} - S_{SC} - (\Delta S)_{IL-M}$ and $V_{SC} \simeq V_M$ as expected near B. This relation leads to a large $(\Delta S)_{M-SC}/(\Delta V)_{M-SC}$, when we take account of the experimental result, $(dP/dT)_{IL-SC} > 0$. Thus, the first-order SC transition with the large $(\Delta S)_{M-SC}/(\Delta V)_{M-SC}$ consistently explains the observed phase diagram with a small dT_c/dP around B. If the M–SC transition is second-order, $(dP/dT)_{IL-SC} = (dP/dT)_{IL-M}$ holds at B, because $(\Delta S)_{M-SC} = 0$ on the M–SC boundary, followed by a rapid decrease in dT_c/dP on cooling along the IL–SC boundary; such behavior was not observed. The first-order SC transition implies some unconventional pairing mechanism, which can be related to the spin-gapped VB ordering.[15] Therefore, it is desired to establish the first-order nature of the SC transition by further experiments.

The global shape of the P–T phase diagram directs our attention to the mean-field phase diagram based on the resonating-valence-bond (RVB) theory for a doped Mott insulator.[16–18] The RVB phase diagram is given with respect to the concentration of the holes generated by doping, while our phase diagram describes the pressure dependence, which corresponds to band width control at half-filling. The Bose condensation line in the RVB phase diagram seems to appear as the IH–M boundary in our P–T phase diagram, although the role of pressure should be distinguished from that of the doping. In the P–T phase diagram, there are two critical points at finite temperatures, A and B, the IH–M–IL and the M–IL–SC critical points, respectively [Fig. 1(c)]. On the other hand, the mean-field RVB phase diagram has one intersecting critical point. Noteworthy is the presence of a spin-gap phase in the proximity of the SC phase in both cases. The highly frustrated IH phase corresponds to the uniform RVB phase.

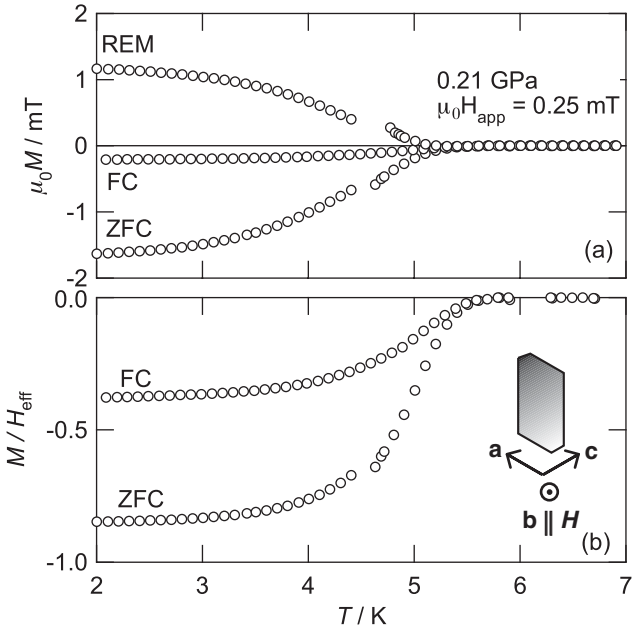

Fig. 2. (a) Magnetization vs temperature of the single crystal at 0.21 GPa for $\boldsymbol{H} \parallel \boldsymbol{b}$. (b) Magnetization corrected for the demagnetizing effect using $N = 0.97$.

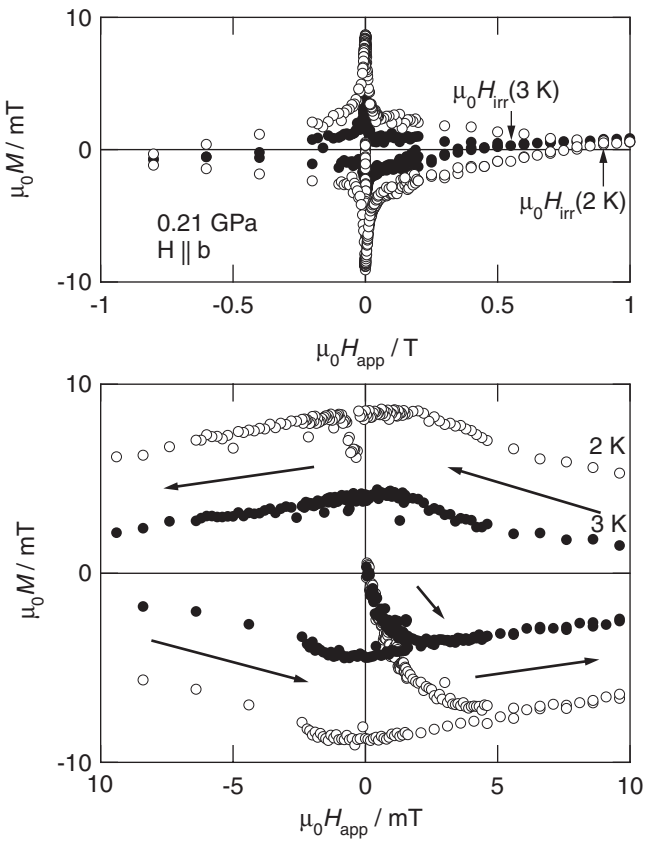

Fig. 3. Field sweep magnetization curve, showing hysteretic loop behavior, taken for the single crystal at 0.21 GPa for $\boldsymbol{H} \parallel \boldsymbol{b}$.

Figure 2(a) shows the $M(T)$ behavior of the single-crystal sample at 0.21 GPa. The data were collected as follows: the sample was first cooled under a zero field to 2.0 K then a field of 0.25 mT was applied. Then, zero-field-cooling (ZFC) data were recorded on heating to 7 K, followed by field-cooling (FC) measurements during cooling to 2.0 K. Next, the field was set to zero again and the remanent magnetization (REM) was measured during heating to 7 K.

The effective field $H_{\rm eff}$ felt by our plate-like single-crystal sample (0.138 mg in weight, $2.0 \times 1.0 \times 0.03\,\mathrm{mm}^3$ in size) should be higher than the applied field $H_{\rm app}$ due to the demagnetization effect, particularly for the field direction normal to the *ac* plane. The demagnetizing effect is expressed as $H_{\rm eff} = H_{\rm app} - NM$, where N is the demagnetizing factor. For a superconductor showing perfect diamagnetism, $M = -H_{\rm eff}$, then we have $H_{\rm eff} = H_{\rm app}/(1-N)$. The demagnetizing factors were roughly calculated by approximating the sample shape by an ellipsoid inscribed in the sample. They are $N_x = 0.010$, $N_y = 0.023$ and $N_z = 0.97$ for the field directions along the principal axes of the ellipsoid, $x > y \gg z$.[19] Therefore, we can assume $H_{\rm eff} \simeq H_{\rm app}$ for the field parallel to the 2D plane, whereas $H_{\rm eff}$ is more than 10 times larger than $H_{\rm app}$ when the field is applied perpendicular to the plane.

For the $\boldsymbol{H} \parallel \boldsymbol{a} + \boldsymbol{c}$ ($\parallel$ 2D layer) measurements, we could observe only small diamagnetic signals, and the linear field dependence was not clear due to the low $H_{\rm c1}$ (see below). Nevertheless, we roughly estimate the magnetization value to be approaching 75% of the perfect diamagnetism at 0.20 GPa. For $\boldsymbol{H} \parallel \boldsymbol{b}$ ($\perp$ 2D layer), we carried out the demagnetization correction using N_z, $H_{\rm app}$, and M values both for the ZFC and FC data. The results are shown in Fig. 2(b). At 2 K, the ZFC shielding value is 85% of the perfect diamagnetism, and the FC Meissner value amounts to 38%; the Meissner-to-shielding ratio is 0.45. Thus, we conclude that the $P2_1/m$ $EtMe_3P$ salt is a bulk superconductor. The sizable remanent magnetization [Fig. 2(a)] is evidence for strong flux pinning. The flux can penetrate into the sample while $\mu_0 H_{\rm c1} < 0.25$ mT, and the temperature is slightly below $T_{\rm c}$. The flux is partly excluded (the Meissner effect) as $H_{\rm c1}$ increases on cooling, but some flux remains due to pinning even after the applied field is removed, so as to give the positive magnetization. If this is the case, $M_{\rm REM} = M_{\rm FC} - M_{\rm ZFC}$ is expected. This is the feature that we find in Fig. 2(a). This also explains the seemingly small Meissner signal.

The hysteretic loop behavior of $M(H)$ showing the type II SC character was recorded at 2 and 3 K under 0.21 GPa (Fig. 3). It is known that, for a 2D superconductor with appreciable vortex fluctuation, the irreversibility field $H_{\rm irr}$, rather than the upper critical field $H_{\rm c2}$, is relevant to the phase boundary under high fields.[20] The $H_{\rm irr}$ values, as defined by the point where the hysteretic behavior disappears, are found to be $\mu_0 H_{\rm irr} = 0.9$ and 0.55 T, at 2 and 3 K, respectively.

The low-field magnetizations at various temperatures are plotted against $H_{\rm eff}$ in Fig. 4(a). From the initial slope, which is common for the 2–4.5 K data, the SC volume fraction is again estimated to be 85% of the perfect diamagnetism. We here define $H_{\rm c1}$ as the field where the magnetization first deviates from the initial linear behavior. According to Bean's critical-state model for the flux entry to superconductors containing pinning centers,[21] the deviation can be expressed as, $\Delta M^{1/2} \propto (H_{\rm eff} - H_{\rm c1})$.[22] In Fig. 4(b), $\Delta M^{1/2}$ is plotted against $H_{\rm eff}$, together with the fit of this formula to the data in the range $0.5 \le \mu_0^{1/2} \Delta M^{1/2} \le 1.0\,\mathrm{mT}^{1/2}$, from which the $H_{\rm c1}$ values are estimated.

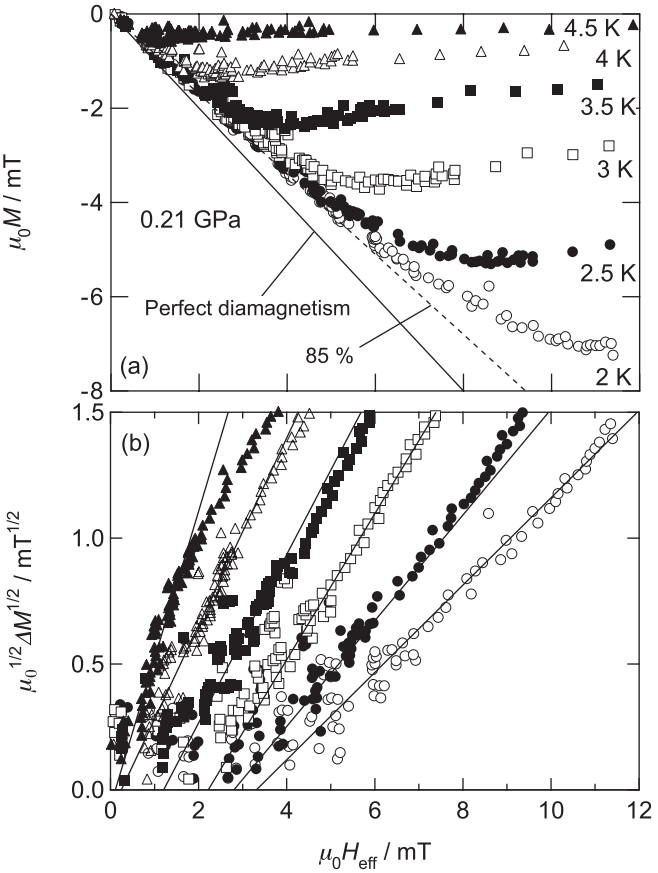

Fig. 4. (a) ZFC Low-field magnetization vs H_{eff}. Solid and broken lines denote 100% and 85% of the perfect diamagnetism, respectively. (b) Square root of the deviation from linearity (the 85% line) vs H_{eff}. Solid lines are the fit of the data to estimate H_{c1}.

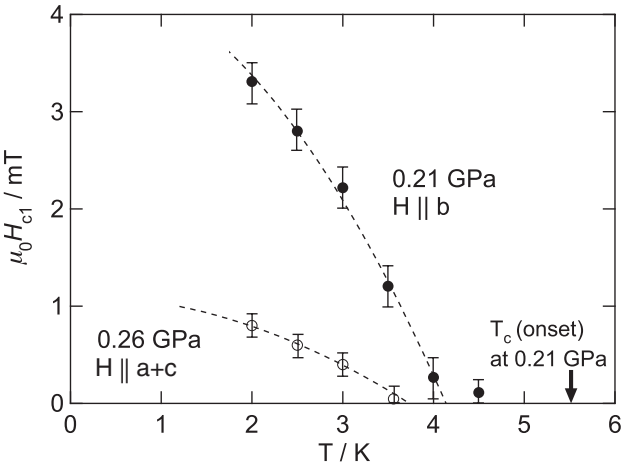

Fig. 5. Temperature dependence of H_{c1}. Dashed curves are the fit using the parabolic law below 4 K.

Figure 5 shows the temperature dependence of H_{c1} thus estimated for $\boldsymbol{H} \parallel \boldsymbol{b}$ ($\perp$ 2D layer) at 0.21 GPa, together with that obtained similarly for $\boldsymbol{H} \parallel \boldsymbol{a} + \boldsymbol{c}$ ($\parallel$ 2D layer) at 0.27 GPa. The temperature dependence of H_{c1} is usually expressed by the parabolic law, $H_{c1}(T) = H_{c1}(0)[1 - (T/T_c)^2]$, when the mean-field approximation is applicable. From the fit of this relation to the data below 4 K, we obtain $\mu_0 H_{c1}(0) = 4.4$ mT and $T_c = 4.1$ K, the latter of which is significantly lower than that estimated by the diamagnetic onset. This is due to a non-parabolic behavior of H_{c1} near T_c, where the vortex fluctuation effect is not negligible.[23] Similar behavior has been reported for other 2D organic superconductors[24,25] and some high-T_c cuprates,[26,27] but a detailed origin is still a controversial issue.[24] The anisotropy of $H_{c1}(0)$ is roughly estimated to be $[H_{c1}(0)]_\perp/[H_{c1}(0)]_\parallel \sim 4$, although the anisotropy measurements were performed at a slightly different pressure. This relatively small anisotropy suggests weak but operating interlayer coupling in the SC state.

In summary, we have established the bulk superconducting behavior of the $P2_1/m$ $EtMe_3P$ salt, for the first time among the [Pd(dmit)$_2$]-based molecular conductors. The temperature-pressure phase diagram has been outlined from the magnetic viewpoint. From the analysis of the field dependence of magnetization, the magnetically critical field values have been estimated.

We thank Dr. A. Fukaya (RIKEN) for the X-ray check of the crystal axes, and Professor M. Imada (Univ. of Tokyo), Professor H. Taniguchi (Saitama Univ.) and Dr. Y. Shimizu (RIKEN) for valuable discussions. This work is supported by Grants-in-Aid for Scientific Research (Nos. 15550135, 16GS0219, and 18043024) from the Ministry of Education, Culture, Sports, Science and Technology, Japan.

1) M. Tamura and R. Kato: J. Phys.: Condens. Matter **14** (2002) L729.
2) M. Tamura and R. Kato: J. Phys. IV **114** (2004) 383.
3) M. Tamura and R. Kato: Polyhedron **24** (2005) 2817.
4) R. Kato: Chem. Rev. **104** (2004) 5319.
5) M. Tamura and R. Kato: J. Phys. Soc. Jpn. **73** (2004) 3108.
6) M. Tamura, Y. Ishii, and R. Kato: to be published in J. Phys.: Condens. Matter **18** (2006).
7) A. Tajima, A. Nakao, and R. Kato: J. Phys. Soc. Jpn. **74** (2005) 412.
8) M. Tamura, A. Nakao, and R. Kato: J. Phys. Soc. Jpn. **75** (2006) 093701.
9) R. Kato, A. Tajima, A. Nakao, and M. Tamura: J. Am. Chem. Soc. **128** (2006) 10016.
10) P. W. Anderson: Science **235** (1987) 1196.
11) S. Ohira, M. Tamura, and R. Kato: Mol. Cryst. Liq. Cryst. **379** (2002) 41.
12) S. Rouzière, N. Hanasaki, R. Kato, and H. Tajima: Solid State Commun. **112** (1999) 295.
13) A. Kobayashi, A. Miyamoto, R. Kato, A. Sato, and H. Kobayashi: Bull. Chem. Soc. Jpn. **71** (1998) 997.
14) Y. Shimizu: private communication.
15) M. Imada: J. Phys. Soc. Jpn. **61** (1992) 423.
16) Y. Suzumura, Y. Hasegawa, and H. Fukuyama: J. Phys. Soc. Jpn. **57** (1988) 2768.
17) T. Tanamoto, H. Kohno, and H. Fukuyama: J. Phys. Soc. Jpn. **61** (1992) 1886.
18) N. Nagaosa and P. A. Lee: Phys. Rev. B **45** (1992) 966.
19) D. Craik: *Magnetism Principles and Applications* (Wiley, Chichester, 1995) p. 93.
20) M. Tinkham: *Introduction to Superconductivity* (Dover, New York, 2004) 2nd ed., Sect. 9.5, p. 334.
21) C. P. Bean: Rev. Mod. Phys. **36** (1964) 31.
22) M. Naito, A. Matsuda, K. Kitazawa, S. Kambe, I. Tanaka, and H. Kojima: Phys. Rev. B **41** (1990) 4823.
23) G. Blatter, B. Ivlev, and H. Nordborg: Phys. Rev. B **48** (1993) 10448.
24) S. Wanka, J. Hagel, D. Beckmann, J. Wosnitza, J. A. Schlueter, J. M. Williams, P. G. Nixon, R. W. Winter, and G. L. Gard: Phys. Rev. B **57** (1998) 3084.
25) S. Wanka, D. Beckmann, J. Wosnitza, E. Balthes, D. Schweitzer, W. Strunz, and H. J. Keller: Phys. Rev. B **53** (1996) 9301.
26) L. Fábrega, B. Martínez, J. Fontcuberta, X. Obradors, and S. Piñol: Phys. Rev. B **46** (1992) 5581.
27) D. A. Brawner, S. Schilling, H. R. Ott, R. J. Haug, K. Ploog, and K. von Klitzing: Phys. Rev. Lett. **71** (1993) 785.